Revisiting the Concept of Equivalence in Solid-State NMR

Frédéric A. Perras & David L. Bryce

University of Ottawa, Ottawa, Ontario, Canada

The concepts of chemical and magnetic equivalence have profound impacts on the understanding and interpretation of NMR phenomena. In solution, magnetic equivalence between spin-1/2 nuclei is generally associated with the lack of an observable spectral *J*-splitting. We examine here the concept of equivalence between quadrupolar nuclei with an emphasis on solid powdered samples. In this context, magnetic equivalence means that the coupled nuclei have identical NMR interaction tensor magnitudes and orientations. Contrary to the spin-1/2 case, J-couplings between magnetically equivalent quadrupolar nuclei are manifested as spectral splittings in solids and in aligned media. Following an overview of the relevant theory, examples employing double-rotation NMR, MQMAS NMR, ultrahigh-field NMR, and two-dimensional *J*-resolved experiments under both spinning and stationary conditions are discussed. The dependence of the observed splittings on the type of equivalence shared by the coupled nuclei (none, chemical, or magnetic) provides a unique experimental handle on crystallographic symmetry, which is of value for structure elucidation.

Keywords: magnetic equivalence, chemical equivalence, quadrupolar nuclei, J-coupling, chemical shifts, *J*-resolved spectroscopy

How to cite this article:
eMagRes, 2015, Vol 4: 561–574. DOI 10.1002/9780470034590.emrstm1469

Introduction

NMR spectroscopy is an immensely powerful analytical technique owing in large part to the impressive and detailed structural insights that may be gleaned through the measurement and interpretation of the fine structure arising from various magnetic and electric interactions involving the nuclei and electrons. The electrons surrounding the nucleus can partially shield it from the applied magnetic field and thus alter its magnetic resonance frequency; this is known as *magnetic shielding* and causes the well-known chemical shift. Nuclei may also magnetically couple among each other either directly, which is known as *direct dipolar coupling* (see ***Dipolar and Indirect Coupling Tensors in Solids***), or through the intervening electrons, which is known as *indirect nuclear spin–spin coupling*, or simply J-coupling (see ***Indirect Nuclear Spin-Spin Coupling Tensors***). Generally, the chemical shift can shed light on the chemical environment of a particular atom, the J-coupling can be used to probe nuclear connectivities, and the dipolar coupling can be directly translated to an internuclear distance in many cases. Clearly, NMR spectra are rich in structural information; however, the spectra are often complicated by the competition of these various interactions. The most thoroughly studied and well understood of these interplays is that between the chemical shift and the J-coupling interactions,[1] as these are the most important NMR interactions that do not average to zero as a result of the rapid isotropic motions of molecules in a liquid. In this article, this situation will first be revisited and the consequences of the symmetry of the system on the behavior of the spin system will also be briefly discussed. More recent developments relating to the impact of chemical and magnetic equivalence on solid-state NMR spectra, particularly in the case of pairs of quadrupolar nuclei, will be described, as well as the response of such spin systems to spin-echo experiments that permit straightforward measurements of dipolar and J-coupling for pairs of quadrupolar nuclei.

Examples and Theoretical Considerations

Pairs of Spin-1/2 Nuclei in Solution

Consider two nuclear spins (I and S), each with a chemical shift, that are J-coupled to each other. The spin Hamiltonian for the system may be written as follows,[2]

$$\hat{H}_{S+J} = \nu_I \hat{I}_Z + \nu_S \hat{S}_Z + J\hat{I}_Z\hat{S}_Z + \frac{1}{2}J(\hat{I}_-\hat{S}_+ + \hat{I}_+\hat{S}_-) \quad (1)$$

where J is the isotropic J-coupling constant and ν_I and ν_S are the chemically shifted resonance frequencies of the nuclei. This Hamiltonian may be reexpressed in matrix form using a basis set composed of Zeeman product states. An example for the simplest case of two spin-1/2 nuclei is shown in equation (2):

$$\hat{H}_{S+J} = \begin{bmatrix} -1/2\,(\nu_I + \nu_S) + 1/4\,J & 0 & 0 & 0 \\ 0 & 1/2(\nu_S - \nu_I) - 1/4\,J & 1/2\,J & 0 \\ 0 & 1/2\,J & 1/2(\nu_I - \nu_S) - 1/4\,J & 0 \\ 0 & 0 & 0 & 1/2(\nu_I + \nu_S) + 1/4\,J \end{bmatrix} \begin{matrix} {}^{-1}/_2, {}^{-1}/_2 \\ {}^{-1}/_2, {}^{1}/_2 \\ {}^{1}/_2, {}^{-1}/_2 \\ {}^{1}/_2, {}^{1}/_2 \end{matrix} \quad (2)$$

As can be seen in equation (2), the matrix is block diagonal and $|{}^{1}/_2, {}^{1}/_2\rangle$ and $|{}^{-1}/_2, {}^{-1}/_2\rangle$ are stationary states. The remaining two states are allowed to mix under the application of the J-coupling Hamiltonian; however, if the difference in chemical shifts between the two spins is large, the difference between ν_I and ν_S will become much larger than the off-diagonal terms, which can then be ignored. Conversely, if the chemical shifts of the two spins are similar, then the $|{}^{1}/_2, {}^{-1}/_2\rangle$ and $|{}^{-1}/_2, {}^{1}/_2\rangle$ states mix, which in turn affects the frequencies of the NMR transitions and their spectral intensities; this is known as an *AB spin system*. Generally, the eigenstates for the two-spin-1/2 case may be written as shown in equations (3) through (6):

$$\psi_1 = |{}^{-1}/_2, {}^{-1}/_2\rangle \quad (3)$$

$$\psi_2 = a\,|{}^{-1}/_2, {}^{1}/_2\rangle + b\,|{}^{1}/_2, {}^{-1}/_2\rangle \quad (4)$$

$$\psi_3 = b\,|{}^{-1}/_2, {}^{1}/_2\rangle - a\,|{}^{1}/_2, {}^{-1}/_2\rangle \quad (5)$$

$$\psi_4 = |{}^{1}/_2, {}^{1}/_2\rangle \quad (6)$$

Determining the values of the mixing coefficients of the eigenstates (a and b) and the energies of the states is relatively straightforward as only the central 2×2 matrix needs to be diagonalized; in the case of more complicated spin systems, numerical diagonalization may be necessary.[1] Similarly, the energies of the different eigenstates are obtained as the eigenvalues from diagonalization. It is then straightforward to calculate the NMR spectrum of such a system as the four transition frequencies may be calculated as differences in eigenvalue energies, and the line intensities may be calculated using the transition probability operator:[1,3]

$$\text{Intensity} \propto \left| \langle n | \sum_{\text{spins}} (I_+ + I_-) | m \rangle \right|^2 \quad (7)$$

The NMR spectra for the classic AB spin system are shown in Figure 1 as a function of the difference in the chemical shifts. The top spectrum, when the chemical shifts of the two nuclei are equal, is that of an A_2 spin system. In this case, the two nuclei cannot be distinguished from one another and the J-coupling between them, while not necessarily zero, no longer has an impact on the NMR spectrum. This can be understood by considering that all the relevant energy levels are increased by $J/4$ in this instance. In the A_2 case, the eigenstates are better described using the total spin wave functions that are defined as $\langle S, M|$, where S is the total spin quantum number and M is the total magnetic quantum number that ranges from $-S$ to S.[2] As the $\langle {}^{1}/_2, {}^{-1}/_2|$ and $\langle {}^{-1}/_2, {}^{1}/_2|$ states are degenerate and indistinguishable, the wave function of the system must also reflect the symmetry imposed by the molecule. Eigenstates that are symmetric and antisymmetric with respect to the exchange of the two spins are then necessary. The appropriate eigenstates are listed in equations (8) through (11).

$$\langle 0,0| = \frac{1}{\sqrt{2}} \left(\langle {}^{1}/_2, {}^{-1}/_2| + \langle {}^{-1}/_2, {}^{1}/_2| \right) \quad (8)$$

$$\langle 1,1| = \langle {}^{1}/_2, {}^{1}/_2| \quad (9)$$

$$\langle 1,0| = \frac{1}{\sqrt{2}} \left(\langle {}^{1}/_2, {}^{-1}/_2| + \langle {}^{-1}/_2, {}^{1}/_2| \right) \quad (10)$$

$$\langle 1,-1| = \langle {}^{-1}/_2, {}^{-1}/_2| \quad (11)$$

These types of spin systems have attracted much attention recently in the literature because the singlet state ($\langle 0,0|$) is not involved in any formally allowed NMR transitions nor is it affected by most of the dominant relaxation mechanisms.[4–8] Singlet states then have very long relaxation times and can be used to store hyperpolarized magnetization over long periods

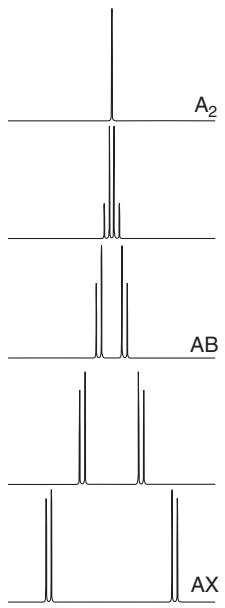

Figure 1. Simulated solution NMR spectra of a pair of J-coupled spin-1/2 nuclei as a function of the ratio of the chemical shift difference to the value of the J-coupling constant. The bottom NMR spectrum represents an AX spin pair, followed by intermediate AB cases, and finally a singlet is observed for the A_2 spin system (top)

of time,[9] which is of particular interest for medical imaging purposes.[10,11]

Symmetry and Magnetic Equivalence

Two spins are magnetically equivalent if they are related by appropriate symmetry elements. A common definition used for solution NMR states that in order for two nuclei to be magnetically equivalent, they must have the same chemical shift and the same J-coupling interactions to all other nuclei external to the pair within the molecule.[12] In the solid state, the two nuclei must also share the same NMR interaction tensor orientations in order for them to be considered magnetically equivalent.[13] Two nuclei with the same tensor magnitudes but differing external spin–spin coupling interactions or tensor orientations are known as *chemically equivalent* (AA′), whereas nuclei with different tensor magnitudes are nonequivalent (AX or AB). The diagrams in Figure 2 show the symmetry operations that are necessary for nuclei to be magnetically or chemically equivalent.

In the solid state, the two coupled nuclei in an AA′ spin system will resonate at different frequencies for each crystallite orientation and thus behave in this respect somewhat as an AX spin system. Under rapid MAS sample rotation, however, the spins appear to behave as an A_2 spin system, whereas at low or intermediate spin rates, AB-type multiplets are observed that have been described as being associated with a J-recoupling interaction.[14−16] This may also be viewed as the $n = 0$ rotational resonance condition. In this sense, higher orders of rotational resonance may be viewed as a partial, experimentally imposed, chemical equivalence.[17]

Nuclei are chemically equivalent if they are related by a symmetry operation such as a reflection, translation, or C_2 rotation (Figure 2b); other symmetry operations that apply to the molecule containing the spins (Figure 2a) do not automatically lead to chemical equivalence. For two nuclei to share the same tensor orientations and be magnetically equivalent, the nuclei must be related either by an inversion center, an improper rotation ($n > 1$), have a rotation axis of order three or higher along the internuclear axis along with a C_2 axis relating the two nuclei, or be related by both a mirror plane and a C_2 axis, as shown in Figure 2c.[13] Although the importance of sharing the same tensor orientations does not affect the NMR spectra of solutions, it does have a clear impact on the lifetime of the singlet state. It has been noted that inversion symmetry was necessary in order for the singlet state in a molecule to be long lived;[18] the other situations in Figure 2c can also be expected to lead to long lived states.

Pairs of Quadrupolar Nuclei in Solution

Quadrupolar nuclei ($I > 1/2$) comprise approximately 3/4 of the NMR-active nuclei including important nuclides such as ^{7}Li, ^{11}B, ^{14}N, ^{17}O, ^{23}Na, ^{27}Al, and ^{35}Cl.[19] The ability to characterize the impact of J-coupling on the NMR spectra of pairs of quadrupolar nuclei could then enable the extraction of much structurally relevant information.[20−23] If we consider a pair of magnetically equivalent spin-3/2 nuclei in solution, the spin system can again be described by equation (1); however, the Hamiltonian in this case may be written as a 16×16 matrix instead of a block-diagonal 4×4 matrix. Similarly to spin-1/2

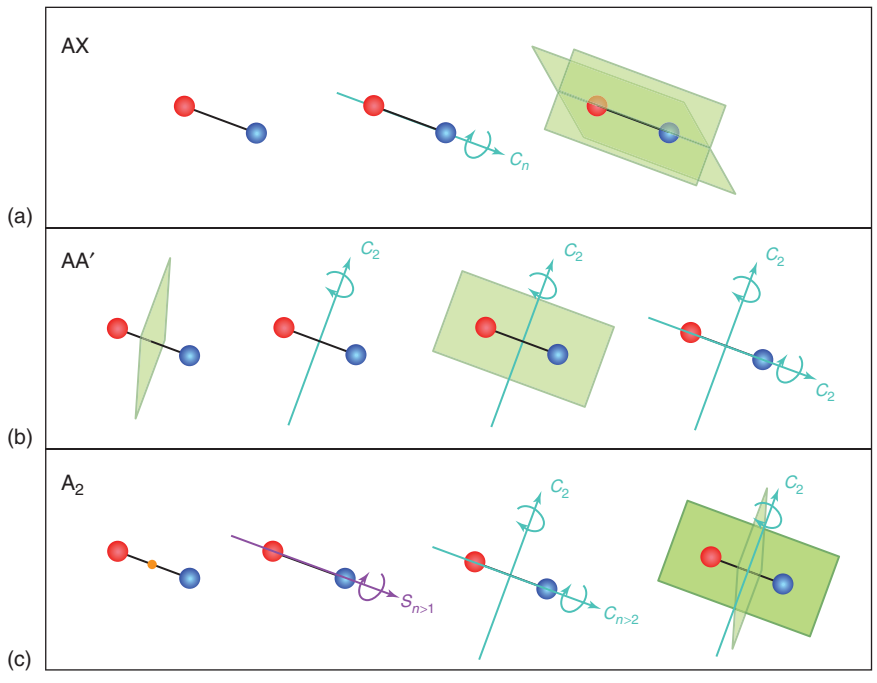

Figure 2. Combinations of symmetry operations for a two-spin system that are consistent with nonequivalence (AX, a), chemical equivalence (AA′, b), or magnetic equivalence (A_2, c) are shown. A green plane represents a mirror plane, a blue arrow represents a rotational symmetry axis, a violet arrow represents an improper rotation axis (note n must be greater than 1), and a yellow dot represents an inversion center. In situations where a molecule contains symmetry operations from multiple rows, the spin system adopts the form characterized by the lowest row

nuclei, the spin system may be described by the total spin eigenstates listed below that were obtained by diagonalizing equation (1) [equations (12) through (27)]:

$$\langle 0,0| = \frac{1}{2}(\langle -3/2,3/2| - \langle 3/2,-3/2| - \langle 1/2,-1/2| + \langle -1/2,1/2|) \quad (12)$$

$$\langle 1,-1| = \sqrt{\frac{2}{5}}\langle -1/2,-1/2| - \sqrt{\frac{3}{10}}(\langle -3/2,1/2| + \langle 1/2,-3/2|) \quad (13)$$

$$\langle 1,0| = \sqrt{\frac{9}{20}}(\langle 3/2,-3/2| + \langle -3/2,3/2|) - \sqrt{\frac{1}{20}}(\langle 1/2,-1/2| + \langle -1/2,1/2|) \quad (14)$$

$$\langle 1,1| = \sqrt{\frac{2}{5}}\langle 1/2,1/2| - \sqrt{\frac{3}{10}}(\langle 3/2,-1/2| + \langle -1/2,3/2|) \quad (15)$$

$$\langle 2,-2| = \frac{1}{\sqrt{2}}(\langle -1/2,-3/2| - \langle -3/2,-1/2|) \quad (16)$$

$$\langle 2,-1| = \frac{1}{\sqrt{2}}(\langle 1/2,-3/2| - \langle -3/2,1/2|) \quad (17)$$

$$\langle 2,0| = \frac{1}{2}(\langle 3/2,-3/2| - \langle -3/2,3/2| + \langle 1/2,-1/2| - \langle -1/2,1/2|) \quad (18)$$

$$\langle 2,1| = \frac{1}{\sqrt{2}}(\langle 3/2,-1/2| - \langle -1/2,3/2|) \quad (19)$$

$$\langle 2,2| = \frac{1}{\sqrt{2}}(\langle 3/2,1/2| - \langle 1/2,3/2|) \quad (20)$$

$$\langle 3,-3| = \langle -3/2,-3/2| \quad (21)$$

$$\langle 3,-2| = \frac{1}{\sqrt{2}}(\langle -1/2,-3/2| + \langle -3/2,-1/2|) \quad (22)$$

$$\langle 3,-1| = \sqrt{\frac{3}{5}}\langle -1/2,-1/2| + \sqrt{\frac{1}{5}}(\langle -3/2,1/2| + \langle 1/2,-3/2|) \quad (23)$$

$$\langle 3,0| = \sqrt{\frac{1}{20}}(\langle 3/2,-3/2| + \langle -3/2,3/2|) + \sqrt{\frac{9}{20}}(\langle 1/2,-1/2| + \langle -1/2,1/2|) \quad (24)$$

$$\langle 3,1| = \sqrt{\frac{3}{5}}\langle 1/2,1/2| + \sqrt{\frac{1}{5}}(\langle 3/2,-1/2| + \langle -1/2,3/2|) \quad (25)$$

$$\langle 3,2| = \frac{1}{\sqrt{2}}(\langle 1/2,3/2| + \langle 3/2,1/2|) \quad (26)$$

$$\langle 3,3| = \langle 3/2,3/2| \quad (27)$$

The energy level diagram for this pair of spins-3/2 is shown in Figure 3, where the energy levels are separated by their total spin. It may be seen clearly that the singlet, triplet, pentet, and septet states are separated from one another, and only the transitions with ΔM of 1 and ΔS of zero are allowed. As for the spin-1/2 case, the singlet state does not participate in any NMR transitions. Additionally, all of the energy levels within a group with the same total spin are affected by the J-coupling Hamiltonian to the same extent; for example, the energies of all seven septet states increase by 9*J*/4, as illustrated in Figure 3. Like the spin-1/2 case, the NMR spectra of pairs of magnetically equivalent quadrupolar nuclei (of any spin) in solution will not be affected by the J-coupling interaction and a single peak will be observed. It may, however, be possible to measure the J-coupling in such systems by performing multiple pulse experiments analogous to the S2M and M2S[24] or SLIC[25] pulse sequences that are used to transfer magnetization in and out of singlet states in the case of spin-1/2 nuclei.[26]

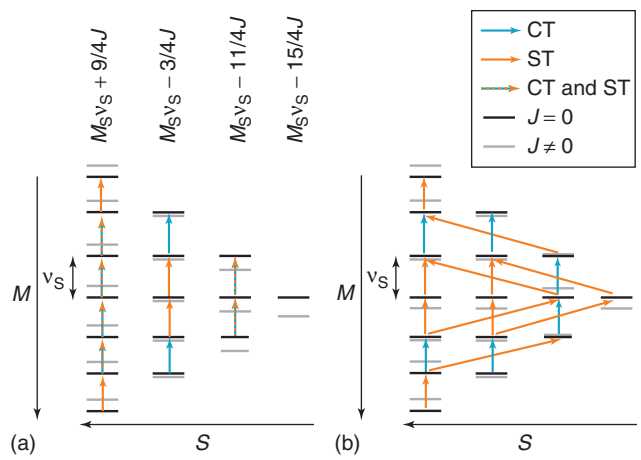

Figure 3. Energy level diagrams for a pair of magnetically equivalent spin-3/2 nuclei with zero quadrupolar coupling (a) or nonzero quadrupolar coupling (b). The energy levels are organized by their total spin (*S*) that increases from 0 to 3, right to left. The black bars indicate the energy levels in the absence of J-coupling and the gray bars indicate how these energy levels are affected by the J-coupling interaction. Yellow arrows represent STs, blue arrows represent the CTs, and the dashed blue and yellow vectors in (a) correspond to transitions that cannot be associated to a particular CT or ST and have mixed contributions from the STs and CTs

Magnetic Equivalence of Quadrupolar Nuclei in Solids or Aligned Media

Unlike spin-1/2 nuclei, quadrupolar nuclei possess a nuclear electric quadrupole moment (Q) that couples with the EFG at the nucleus. This quadrupolar interaction perturbs the Zeeman energy levels, as described by the following Hamiltonian equation (28), and is often much stronger than the other internal NMR interactions (see ***Quadrupolar Interactions***):

$$\hat{H}_{\mathrm{Q}} = \frac{eQ}{6I(2I-1)}\mathbf{I}\cdot\mathbf{V}\cdot\mathbf{I} \qquad (28)$$

In the above expression, e represents the fundamental charge, $\mathbf{I}$ is the nuclear spin angular momentum vector, and $\mathbf{V}$ is the EFG tensor. $\mathbf{V}$ is traceless and symmetric and is thus typically parameterized using only the quadrupolar coupling constant ($C_{\mathrm{Q}} = eQV_{33}/h$, where V_{33} is the largest component of $\mathbf{V}$) and the quadrupolar asymmetry parameter ($\eta = (V_{11} - V_{22})/V_{33}$). The quadrupolar interaction does not directly contribute to the NMR spectrum in solution but does have pronounced effects on the NMR line shape in the case of solid powdered samples. The quadrupolar Hamiltonian expressed as a first-order perturbation to the Zeeman interaction is given in equation (29):

$$\hat{H}_{\mathrm{Q}}^{(1)} = \frac{C_{\mathrm{Q}}(3\hat{I}_z^2 - \hat{I}^2)}{8I(2I-1)}[(3\cos\theta - 1) + \eta\sin^2\theta\cos 2\varphi] \qquad (29)$$

In equation (29), θ represents the angle between the applied magnetic field and the orientation of V_{33} (which is fixed in the molecular frame) and φ is the second polar angle describing the orientation of the EFG tensor within the laboratory frame. The dependence of the NMR frequency on the orientation of the crystallite indicates that broad powder patterns are expected in the NMR spectra of solid powdered samples. The central transition (CT, $m = 1/2$ to $-1/2$) is, however, unaffected by the quadrupolar interaction to first order and thus remains relatively sharp even in powdered samples. Most NMR experiments on half-integer quadrupolar nuclei focus solely on the detection and interpretation of the CT. The satellite transitions (ST) are separated from the CT by the first-order quadrupolar coupling. The splitting ($\Delta\nu_{\mathrm{Q}}$) between adjacent resonances is orientation-dependent and varies with the size of the quadrupolar coupling constant as follows [equation (30)]:

$$\Delta\nu_{\mathrm{Q}} = \frac{3C_{\mathrm{Q}}}{2I(2I-1)}[(3\cos\theta - 1) + \eta\sin^2\theta\cos 2\varphi] \qquad (30)$$

Note that here the splitting represents the difference between the adjacent transitions' frequencies, as opposed to the splitting between pairs of STs $m \rightarrow m-1$ and $-m \rightarrow -(m-1)$ (as given in Abragam[27]), and thus does not depend to first-order on the value of m.

The impact of the first-order quadrupolar interaction is to lift the degeneracy of the various levels with equal values of Σm in the two-spin case. Unlike in solution, where all states with equal Σm are allowed to mix, when a first-order quadrupolar interaction is present, only the states defined by permutations of the same Zeeman m states are allowed to mix. For example, as they are no longer degenerate, the $\langle 3/2, -3/2|$ and $\langle 1/2, -1/2|$ states can no longer mix. The $\langle 3/2, -3/2|$ and $\langle -3/2, 3/2|$ states must nonetheless remain mixed in order to reflect the symmetry of an A_2 spin system. The spin system is then defined by a new set of eigenstates that are analogous to the total spin wave functions presented earlier [equations (12) to (27)]. These states are organized into groups with symmetric and antisymmetric combinations of the Zeeman product states for eigenstates with identical permutations of the same m values [equations (31) and (32)].[28]

$$\frac{1}{\sqrt{2}}(|m_1, m_2\rangle + |m_2, m_1\rangle) \qquad (31)$$

$$\frac{1}{\sqrt{2}}(|m_1, m_2\rangle - |m_2, m_1\rangle) \qquad (32)$$

The energy level diagram for an A_2 pair of spins-3/2 in noncubic solids is shown alongside the solution-state energy level diagram in Figure 3. It can be seen that in the presence of quadrupolar coupling, there are now well-defined CTs and STs. Additionally, in this case, some of the allowed STs occur between states with a change in total spin of ± 2. This effect means that in the presence of a quadrupolar splitting, the singlet state is no longer isolated. All of the commonly observed CTs, however, do not involve a change in total spin.[29]

It was predicted in 1967 by Saupe and Nehring, and also by Musher, that the magnetic equivalence of quadrupolar nuclei would be broken in liquid crystals and that the J-coupling would become measurable.[30,31] They noted that the total spin states [equations (12) through (27)] are no longer valid in an anisotropic medium and that the homonuclear J-coupling in D_2 would be measurable; see Ref. 32 for a discussion and experimental demonstration.

It can also be noticed from the energy level diagram in Figure 3 that the energy levels within a given group with equal total spin are no longer affected equally by the J-coupling interaction. The CT NMR spectrum would then be composed of multiplets, and the homonuclear J-coupling for a quadrupolar A_2 spin system would affect the solid-state NMR spectrum. The expected CT multiplets for high-resolution NMR spectra of quadrupolar nuclei in solids or aligned liquids are depicted in Figure 4.[28,29]

For simplicity, the A_2 multiplets depicted in Figure 4 can be decomposed into a series of individual doublets for every possible $|m|$ value for the coupled nucleus (m is the magnetic quantum number). Most of these doublets are split by $2mJ$, as would also be the case for AX spin systems. If the value of m of the coupled nucleus is $\pm 3/2$ or $\pm 1/2$, the last term in the J-coupling Hamiltonian equation (1) is nonzero and the splitting is altered. For the CT among the symmetric states [equation (31)] when $m = \pm 3/2$, the splitting of the doublet is given by $(I^2 + I + 9/4)J$, whereas the splitting for the CT in the antisymmetric states [equation (32)] is $(2I + 5)(2I - 3)J/4$. These two doublets have half the intensity of the others as the intensity is distributed over both of the transitions. Lastly, when both spins are in a symmetric central state (pseudo-triplet states) the splitting of the doublet, within the greater multiplet, is equal to $(2I + 3)(2I - 1)J/4$ (see Figure 4).[28]

The previously considered case of magnetically equivalent quadrupolar nuclei with zero quadrupolar coupling may also

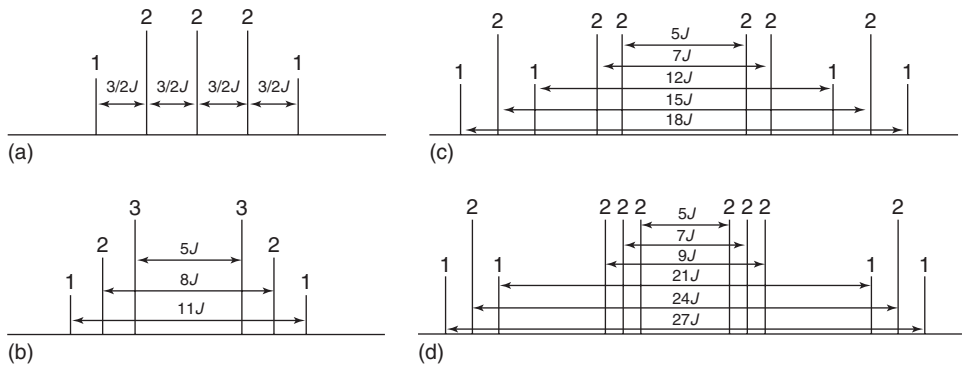

Figure 4. First-order, CT-only, J-coupling multiplets for A_2 spin pairs of half-integer quadrupolar nuclei. The multiplets for a pair of spin-3/2, 5/2, 7/2, and 9/2 nuclei are shown in (a), (b), (c), and (d), respectively. The line splittings are indicated using double-headed arrows, and the relative intensities of the lines are marked above the resonances. (Adapted from J. Magn. Reson., 242, F. A. Perras and D. L. Bryce, Theoretical study of homonuclear J-coupling between quadrupolar spins: Single-crystal, DOR, and J-resolved NMR, 23–32, Copyright (2014), with permission from Elsevier)

be thought of as a situation where the STs resonate at the same frequency as the CT and are thus mutually equivalent. We have referred to these as central-satellite magnetically equivalent (CS-A_2) spin systems.[28] When the splitting, which separates the STs from the CT, is large when compared to the J-coupling, the CT and STs no longer mix and the spin system is described by the A_2 case from equations (31) and (32). As the J-coupling is typically small when compared to the quadrupolar coupling and a quadrupolar splitting as small as 6 kHz is large enough to break the CS-A_2 symmetry in a diboron spin pair ($J(^{11}B,^{11}B) \sim 100$ Hz), the A_2 multiplets shown in Figure 4 should be expected for magnetically equivalent pairs of quadrupolar nuclei in most practical situations. Numerical simulations showing the spectral changeover from the CS-A_2 to the A_2 case are shown in Figure 5a.

As the distinction between the CS-A_2 and A_2 cases originates from the splitting caused by the first-order quadrupolar interaction, a special situation would also arise in the case of chemically equivalent spin pairs (i.e., AA′ spin systems). Chemically equivalent nuclei have the same tensor magnitudes and chemical shifts but differ in their tensor orientations [θ and φ in equation (30)]. Even slight differences in the tensor orientations (a few degrees or less) would break the equivalence of the STs of the coupled nuclei owing to a large difference in their quadrupolar splittings. The CTs, however, which are only affected by the quadrupolar interaction to second order, would remain practically equivalent for the two nuclei, unless there is a large second-order quadrupolar shift difference. The doublets originating from the coupling of a $m = \pm 1/2$ state to a $\pm 3/2$ state, which are a part of the A_2 multiplet, would have a splitting of $3J$ as opposed to $(I^2 + I + 9/4)J$ and $(2I + 5)(2I - 3)J/4$. As the central transitions would nonetheless remain equivalent amongst each other, the splitting from the doublet of the central states would remain equal to $(2I + 3)(2I - 1)J/4$.[28] This situation is analogous to the case of rapidly spinning pairs of spin-1/2 nuclei for which only a single resonance is observed as they behave like an A_2 spin system.[14] An example of spectral changeover from the A_2 to the AA′ multiplet for a pair of chemically equivalent spin-3/2 nuclei is shown in Figure 5.

As described here, in the case of quadrupolar nuclei, a rich diversity of different multiplets is expected owing to the presence of the first-order quadrupolar interaction which is absent for spin-1/2 nuclei. Namely, CS-A_2, A_2, AA′, and AX spin systems all give rise to distinct, first-order, multiplet structures. Importantly, these would only typically be observable in cases when the second-order quadrupolar interaction does not obscure the fine structure. For example, these types of multiplets would be observable in cases of very high magnetic fields, single crystals, partially aligned liquids, and samples that are spun simultaneously about two angles, a technique known as *double-rotation* (DOR),[33] to average the second-order quadrupolar interaction. The J-coupling information could also be extracted with the use of tailored multiple pulse experiments that are sensitive to the J-coupling and remain unaffected by the second-order quadrupolar interaction. Experimental measurements of homonuclear spin–spin coupling in quadrupolar A_2 spin pairs will be discussed in the following sections.

High-Resolution Solid-State NMR

The narrower CT is not affected by the first-order quadrupolar interaction but it is broadened to second order. The broadening caused by this interaction depends inversely on the magnetic field strength and directly on the square of the C_Q value (see ***Quadrupolar Interactions***; ***Quadrupolar Nuclei in Solids: Influence of Different Interactions on Spectra***). Unlike the first-order quadrupolar interaction, dipolar coupling, and chemical shift anisotropy, the second-order nature of this interaction means that it cannot be averaged to zero by rapid sample rotation about the magic angle ($\theta = 54.74^\circ$). In fact, the second-order quadrupolar broadening depends on both the second- and fourth-order Legendre polynomials of $\cos\theta$. In order to remove this broadening one may spin the sample about two angles simultaneously (i.e., DOR)[33] or sequentially (dynamic angle spinning, DAS).[34] In order to observe the multiplets shown in Figure 4, the use of such a high-resolution technique, or very high magnetic fields, is necessary.[35]

The ^{11}B ($I = 3/2$) and ^{55}Mn ($I = 5/2$) DOR NMR spectra of bis(catecholato) diboron and dimanganese decacarbonyl have

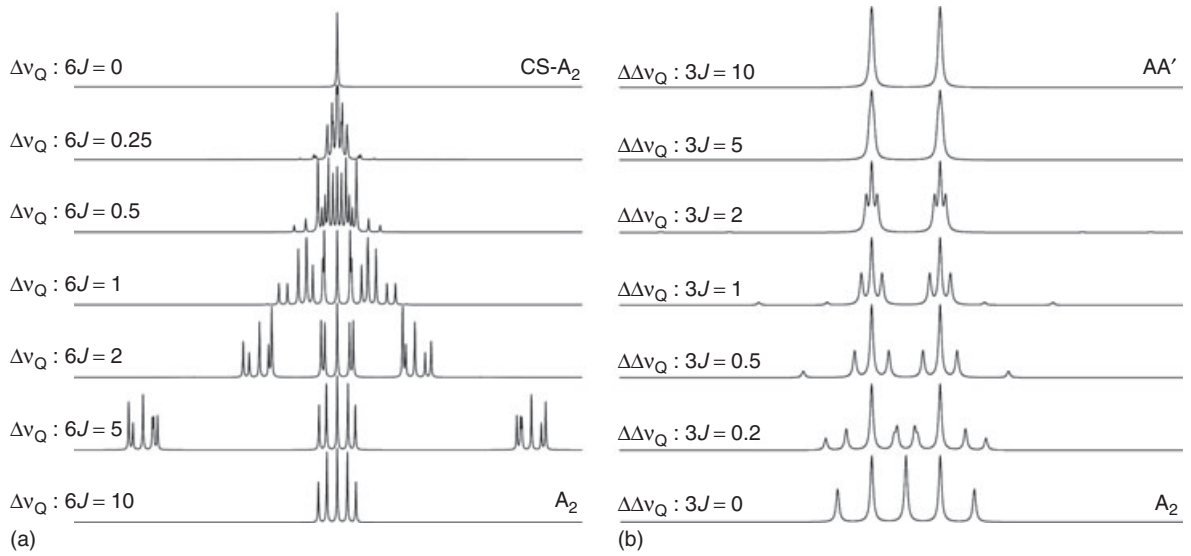

Figure 5. The spectral changeover from A_2 to CS-A_2 multiplets is shown in (a). The CT multiplet is greatly affected as the ST resonances approach the CT resonances and eventually collapses to a singlet. The spectral changeover from the A_2 to the AA′ case is shown in (b). The doublet with a splitting of $3J$, originating from the central states of both spins, is unaffected, whereas the other resonances converge to a splitting of $3J$ in the AA′ case. (Adapted from J. Magn. Reson., 242, F. A. Perras and D. L. Bryce, Theoretical study of homonuclear J-coupling between quadrupolar spins: Single-crystal, DOR, and J-resolved NMR, 23–32, Copyright (2014), with permission from Elsevier)

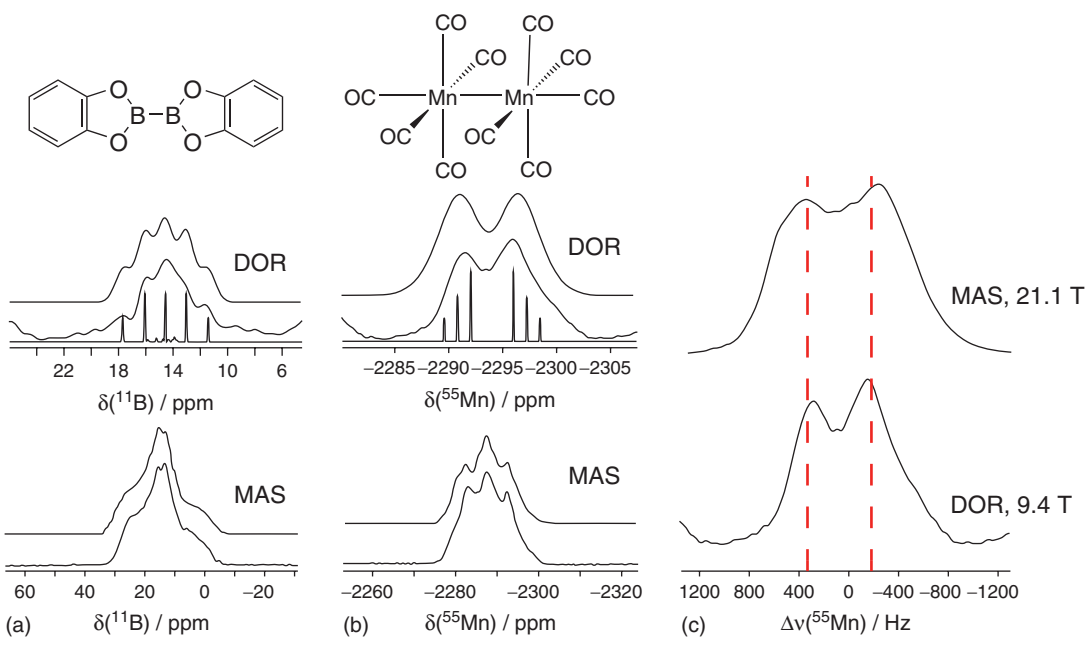

Figure 6. (a) The ^{11}B MAS (bottom) and DOR (middle) NMR spectra of bis(catecholato) diboron (structure on top) are shown. The ^{55}Mn MAS and DOR NMR spectra of dimanganese decacarbonyl are shown in (b). Simulations of the MAS spectra and the DOR spectra (with and without line broadening) are overlaid with the experimental spectra. In (c) the ^{55}Mn DOR (9.4 T) and MAS (21.1 T) NMR spectra are overlaid showing the magnetic field independence of the splitting. (Adapted with permission from F. A. Perras, D. L. Bryce, J. Chem. Phys. 2013, 138, 174202. Copyright 2013, AIP Publishing LLC)

been acquired at a magnetic field strength of 9.4 T;[29] these spectra are shown in Figure 6. It is evident in Figure 6a that the ^{11}B MAS NMR spectrum of bis(catecholato) diboron is mainly affected by the second-order quadrupolar interaction and that the effects of the J-coupling are not obvious. The ^{11}B DOR NMR spectrum, however, reveals a centerband that is split into a multiplet consisting of five individual lines with approximately the expected line intensities of 1 : 2 : 2 : 2 : 1; these intensities are distributed across the spinning sidebands and are not expected to be perfectly reproduced in the centerband. From this DOR

NMR spectrum a $J(^{11}B,^{11}B)$ value of 130 ± 20 Hz may be measured.

In the case of dimanganese decacarbonyl, the MAS NMR spectrum is unusual and is more obviously affected by both the J-coupling and the second-order quadrupolar interaction.[36] DOR experiments on this sample clearly reveal the J-coupling fine structure.[29] The six lines that are expected for the spin-5/2 A_2 multiplet are not resolved but a doublet with a splitting that should be approximately equal to $5J$ is observed. The multiplet may be simulated in order to extract the $J(^{55}Mn, ^{55}Mn)$ coupling constant of 100 ± 20 Hz.

The ^{55}Mn MAS NMR spectrum of dimanganese decacarbonyl has also been acquired at 21.1 T where the effects of the J-coupling are expected to dominate the spectral line shape owing to the inverse dependence of the second-order quadrupolar interaction on the magnetic field strength. This NMR spectrum is displayed along with the DOR NMR spectrum acquired at 9.4 T in Figure 6c. The MAS line shape at 21.1 T resembles the DOR NMR line shape but is slightly broader owing to the nonzero effects of the second-order quadrupolar interaction. Analogous A_2 multiplets can also be measured in single crystals, where the effects of dipolar coupling will also be present, as well as in partially aligned liquids.[32] A related case for chemically equivalent deuterons ($I = 1$) in solids has also been presented.[37]

Another high-resolution technique has made it possible to measure J-coupling between magnetically equivalent quadrupolar nuclei in solids, the MQMAS experiment.[38] In the MQMAS experiment, the sample is spun at the magic angle to average the first-order broadening, and the second-order quadrupolar interaction is refocused in a 2D experiment by letting the signal evolve through both single and triple quantum coherences.[39,40] In the presence of J-coupling, it is necessary to consider the evolution of the J and quadrupolar coupling through the triple quantum coherence (3/2 to −3/2 transition) and the CT coherence in order to simulate the multiplets expected in the high-resolution dimension.[38] These multiplets are not identical to those that are depicted in Figure 4 and are likely to depend on many experimental and internal factors. Time consuming powder averaged density matrix simulations are then necessary in order to extract the spin–spin coupling information from the NMR spectra. This approach, however, does not require the use of specialized probe hardware. The ^{11}B and ^{55}Mn MQMAS NMR spectra of bis(pinacolato) diboron and dimanganese decacarbonyl are shown in Figure 7 along with their simulations. As can be seen, the isotropic dimensions do indeed show multiplet structures because of the spin–spin coupling in the A_2 spin pairs but the multiplets cannot be analyzed as simply as in the DOR or high-field MAS spectra.

J-Resolved NMR Spectroscopy

J-coupling constants typically may be measured with much higher precision using a two-dimensional experiment known as the *J-resolved experiment*.[41] In the basic J-resolved experiment a Hahn echo ($p(90^\circ) - t_1/2 - p(180^\circ) - t_1/2 -$ acq.) is performed and the echo delay ($t_1/2$) is incremented. The 180° pulse reverses the effects of the chemical shift interaction such that after the second delay its effects are absent. The J-coupling, however, is not refocused by the 180° pulse and continues to evolve during the second t_1 period.[42,43] A Fourier transform along t_1 gives the J-coupling multiplet, without the effects of other interactions, with high resolution as the broadening caused by inhomogeneous magnetic fields (and distributions of chemical shifts in solids) are fully refocused and the line width is dictated by the relaxation time constant, T_2.

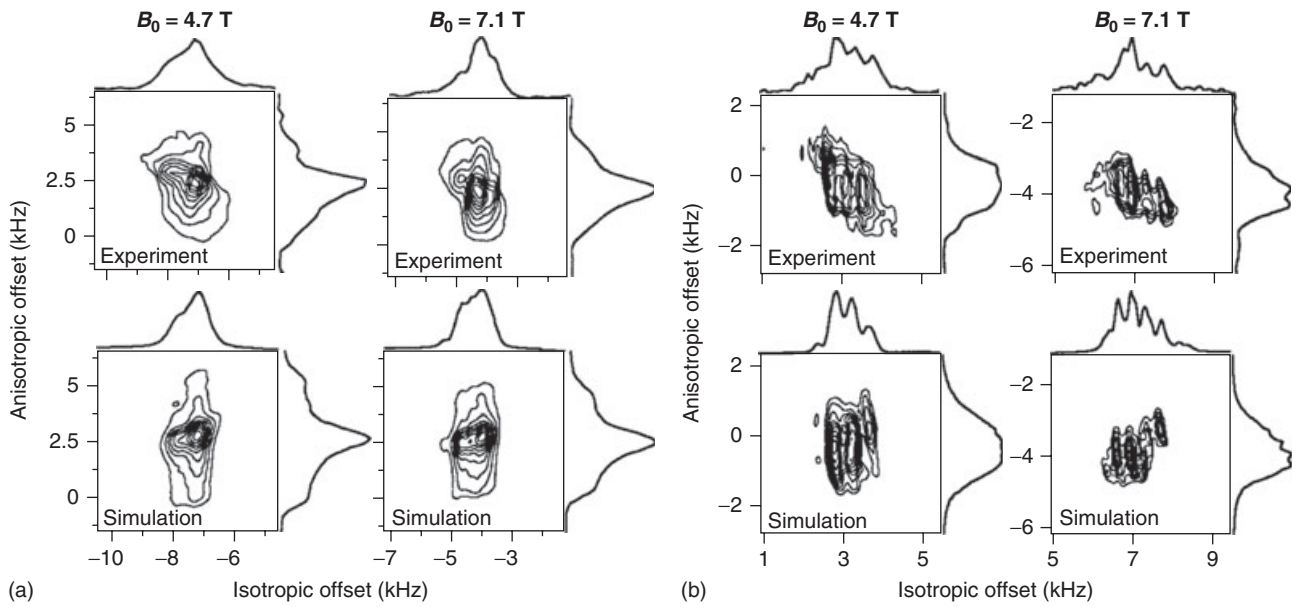

Figure 7. The experimental and simulated ^{11}B and ^{55}Mn MQMAS NMR spectra of bis(pinacolato) diboron (a) and dimanganese decacarbonyl (b) are shown. The spectra have been acquired at two different applied magnetic field strengths of 4.7 and 7.1 T. (Reprinted with permission from S. Wi, L. Frydman, J. Chem. Phys. 2000, 112, 3248–3261. Copyright 2000, AIP Publishing LLC)

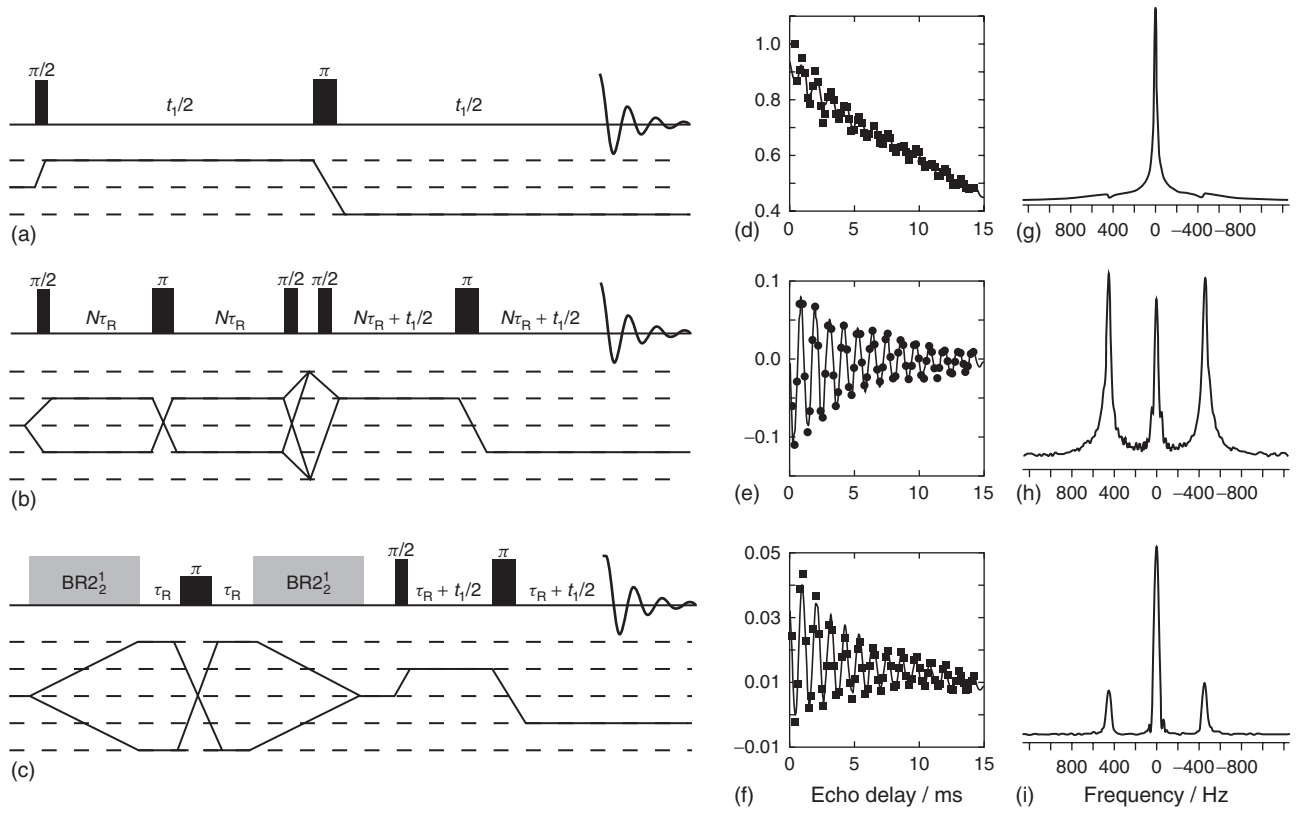

Figure 8. *J*-resolved solid-state NMR experiments for half-integer spin quadrupolar nuclei. Pulse sequences for the regular, *J*-DQF, and dipolar-DQF *J*-resolved experiments are shown in (a), (b), and (c), respectively; coherence transfer pathways are shown below the pulse schemes. The modulations of the echo intensities as a function of the echo delay for ^{55}Mn in dimanganese decacarbonyl subjected to each of the three experiments are shown in (d), (e), and (f), and the Fourier transforms of these signals are shown in (g), (h), and (i). (Reproduced with permission from Ref. 44. © American Chemical Society, 2013)

It has recently been demonstrated that *J*-resolved experiments are also amenable to half-integer quadrupolar nuclei.[44] In this case, however, only the CT can be manipulated with the necessary level of precision using low power, CT-selective, pulses (pulse lengths scaled by $1/(I+1/2)$). As the J-coupling can only modulate the signal intensity in a Hahn echo experiment if both spins are inverted by the 180° pulse, only the transitions involving pairs of nuclei in $m \pm 1/2$ states can modulate the NMR signal. This is unfortunate because only $1/(I+1/2)$ of the NMR signal can be used to measure the J-coupling; however, a much simpler multiplet structure is expected in the indirect dimension of a 2D *J*-resolved experiment on quadrupolar nuclei than those depicted in Figure 4.[28]

Most of the signal is perfectly refocused by the 180° pulse, which leads to a large resonance at zero frequency in the Fourier transform of the spin-echo modulation. The signal arising from a $m = \pm 1/2$ state that is coupled to another central state would however be modulated and lead to the formation of a doublet in the *J*-resolved spectrum. The splitting of this doublet is equal to its corresponding splitting within the multiplet in the 1D DOR NMR spectra. In AA′ or AX cases, the splitting of the doublet is given simply by the J-coupling constant, whereas this splitting is amplified by $(2I+3)(2I-1)/4$ if the spins are magnetically equivalent. This amplification factor corresponds to 0, 3, 8, 15, and 24 for pairs of nuclei of spin 0, 3/2, 5/2, 7/2, and 9/2, respectively. The pulse sequence and a sample ^{55}Mn *J*-resolved NMR spectrum are shown in Figure 8.

As is evident from the spectrum in Figure 8g, the main resonance at zero frequency can be quite burdensome and could hinder the measurement of small J-coupling constants. This resonance can, however, be suppressed with the use of a CT-selective double-quantum filter (DQF) because only the signals from spin pairs where both spins are in the central states would survive. We have proposed two separate DQF schemes utilizing either the J-coupling (with a refocused INADEQUATE block,[45] Figure 8b) or the dipolar coupling (with a symmetry-based, $BR2_2^1$,[46] recoupling block, Figure 8c) to excite the two-spin double-quantum coherences. With these experiments, only a single doublet is expected for every spin pair, the splitting of which provides insights into the symmetry of the molecule as an amplified splitting is expected for the A_2 case, whereas a splitting of *J* is expected in the AX or AA′ cases (see Figure 9a).

A number of diboron systems have been studied using this methodology,[47] and some of their DQF-*J*-resolved spectra are shown in Figure 9. Many of these diboron compounds possess a crystallographic inversion center relating the two boron nuclei and thus exhibit large $J(^{11}B,^{11}B)$ splittings consistent with the amplification factor described earlier. Tetrakis(pyrrolidino) diboron, however, has a nonzero N–B–B–N dihedral angle and thus nonmagnetically equivalent boron sites,[48] and features the

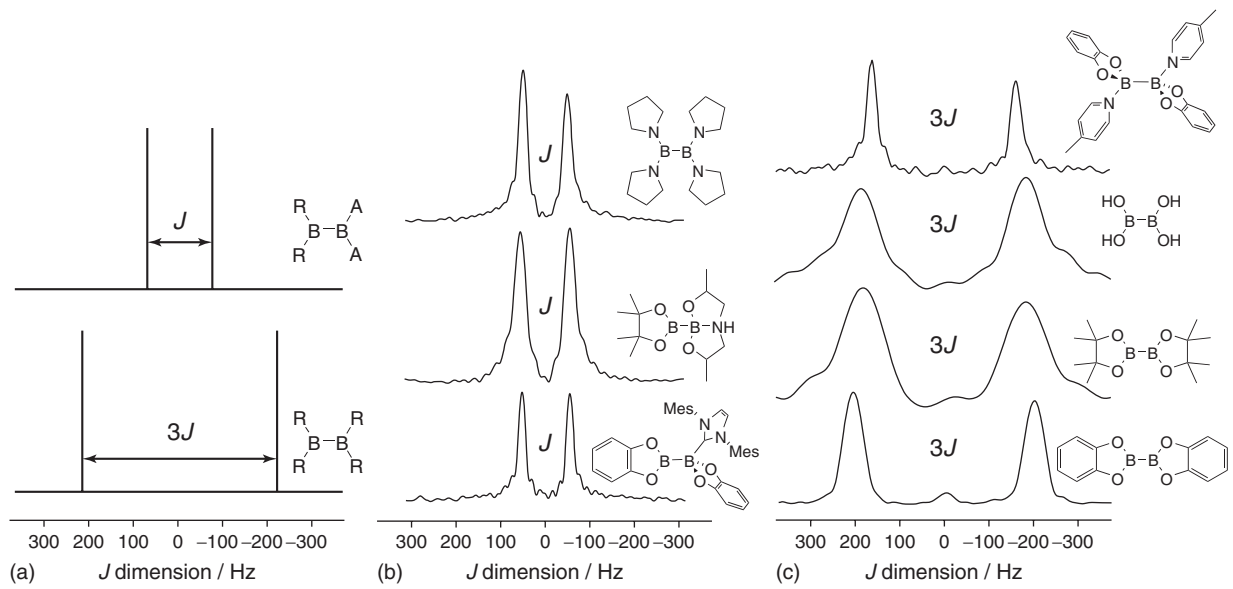

Figure 9. (a) The expected *J*-resolved multiplets for AX and A_2 spin pairs of ^{11}B nuclei are shown. In (b) and (c) experimental *J*-resolved spectra of diboron compounds without inversion symmetry (b) and with inversion symmetry (c) are shown along with the structures of the compounds in question. (Reproduced from F. A. Perras, D. L. Bryce, Chem. Sci. 2014, 5, 2428–2437. Published by The Royal Society of Chemistry)

smallest of the *J* splittings observed in that study (98 ± 2 Hz).[47] Many diboron compounds of interest in β-boration chemistry also exist, some of which have been investigated and feature nonamplified splittings owing to the low symmetry of the molecules. The symmetry amplification of the *J* splittings in the case of magnetically equivalent spin systems has also been exploited in order to detect a small, two-bond, J-coupling between two ^{11}B nuclei in 9-BBN.[47]

It is important to note additionally that the second-order quadrupolar-dipolar cross-term does not affect the splittings in a *J*-resolved NMR experiment.[28] The cross-term interaction only depends on the square of *m*, and thus the $\pm 1/2$ states are affected equally and the cross-term is refocused by the 180° pulse.

Static *J*/*D*-Resolved NMR Spectroscopy

The NMR experiments described earlier are particularly exciting as they provide a clear separation of the spin–spin coupling interactions from the chemical shift and quadrupolar coupling interactions, the last of which is often overwhelming in size, with the use of a simple Hahn echo experiment. However, these experiments rely on the use of MAS or DOR to provide resolution, which is often impractical for nuclei with very strong quadrupolar interactions. Instead, *J*-resolved experiments may be performed under stationary conditions where both the dipolar coupling and the J-coupling would affect the *J*-resolved dimension. The spin–spin coupling Hamiltonian, in the static case, may be written as follows [equation (33)]:

$$\hat{H}_{D+J} = (J + d)\hat{I}_z\hat{S}_z + (J/2 - d/4)(\hat{I}_+\hat{S}_- + \hat{I}_-\hat{S}_+) \qquad (33)$$

where *d* is given by equation (34):

$$d = -R_{eff}(3\cos^2\theta - 1) \qquad (34)$$

R_{eff} corresponds to the effective dipolar coupling constant ($R_{eff} = R_{DD} - \Delta J/3$; ΔJ is the anisotropy of the J-coupling tensor) and θ is the angle between the magnetic field and the internuclear vector. This Hamiltonian determines the modulation frequency of a static Hahn echo modulation experiment; note that only the states where both spins have *m* values of $\pm 1/2$ are modulated, such as in the MAS case.[44] As only the first term in equation (33) is nonzero for the AX case, the static *J*/*D*-resolved modulation frequency is given by $\pm 1/2(J + d)$ and a split Pake doublet would be obtained. If equations (31) and (32) are used, for the A_2 case, then the modulation frequency is amplified as follows:

$$\nu_{D+J} = \frac{(2I + 3)(2I - 1)J}{8} - \frac{(I^2 + I + 9/4)d}{4} \qquad (35)$$

The dipolar splittings are then amplified by a factor of −3/2, −3, −11/2, −9, and −27/2 for pairs of nuclei of spin 1/2, 3/2, 5/2, 7/2, and 9/2, respectively. It is interesting to note that the sign of the dipolar modulation is reversed in the A_2 case which would lead to an opposite sense for both halves of the Pake doublet powder patterns in a static *J*/*D*-resolved NMR experiment (see Figure 10).[49]

In order to perform static *J*/*D*-resolved NMR experiments, the intensity losses from the application of a DQF may no longer be justified as it would also lead to distortions in the line shapes. As the duration of the FID is particularly short in static cases, we have instead proposed a much more sensitive shifted-echo experiment which would provide higher resolution undistorted line shapes, albeit without the suppression of the large resonance at zero frequency. The shifted-echo procedure ensures that pure phase 2D line shapes are obtained.[50] As the experiment is essentially a Hahn echo, it is amenable to cases where sensitivity may be an issue.

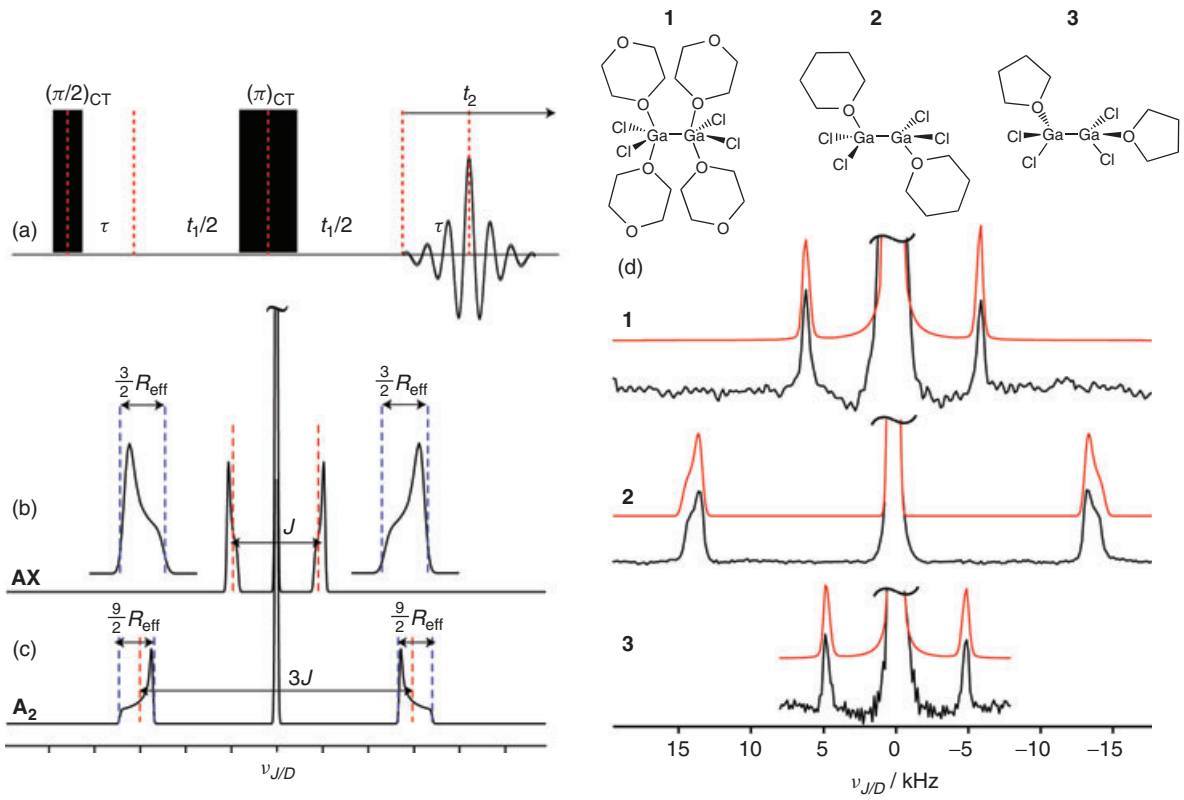

Figure 10. The shifted-echo *J*/*D*-resolved pulse sequence is shown in (a) and the expected theoretical spectra are shown in (b) and (c) for AX and A_2 pairs of spin-3/2 nuclei, respectively. Experimental static *J*/*D*-resolved NMR spectra are shown in (d) for a series of digallium compounds pictured and numbered over the spectra; the middle compound (**2**) has magnetically equivalent gallium species, as is evident from the amplified splitting and the inverted sense of the Pake-like patterns. (Reprinted with permission from F. A. Perras, D. L. Bryce, J. Phys. Chem. Lett. 2014, 5, 4049−4054. Copyright (2014) American Chemical Society)

This experiment has been performed on a series of digallium compounds ($I(^{71}\mathrm{Ga}) = 3/2$) that have quadrupolar coupling constants ranging from 31.4 to 46 MHz and CT line widths exceeding 1 MHz at an applied magnetic field strength of 21.1 T.[49] As the bandwidth of the square pulses is limited, the 2D NMR experiment was performed on a piece of the full CT powder pattern.[51] It can be seen from the spectra in Figure 10d that one of the compounds (the THP species) possesses magnetically equivalent gallium nuclei, as is evident from the amplified splitting and the sense of the powder patterns, enabling the elucidation of the 3D structure of this species whose crystal structure is unknown. This static *J*/*D*-resolved NMR experiment is far simpler and easier to interpret than some other methods that have been proposed for measuring dipolar coupling between quadrupolar nuclei,[52,53] and can even be applied to cases where the quadrupolar interaction is so large that the NMR spectrum cannot be acquired in a single piece.[54]

Conclusion

The concept of equivalence is of profound importance in NMR owing to its direct impact on NMR spectra. While this concept is well understood and applied in solution NMR spectra of spin-1/2 nuclei, we have described in this article some of the interesting manifestations of J-coupling between magnetically equivalent quadrupolar nuclei in solids. It has long been known that the equivalence of nuclear spins could be broken in liquid crystals when the Hamiltonian does not have permutation symmetry.[12] Spin–spin coupling is thus measurable in liquid crystals for magnetically equivalent pairs of quadrupolar nuclei.[30−32]

In solution, the lack of observable mutual coupling between spins goes hand-in-hand with the concept of magnetic equivalence. The Devil's Advocate may consider the fact that *J* splittings are indeed observable for pairs of magnetically equivalent quadrupolar spin pairs in liquid crystals and solids as an indication that there is no such thing as magnetically equivalent quadrupolar spin pairs; however, in this article, we have been careful to point out what is meant by magnetic equivalence in the solid state: the nuclei considered must have identical NMR tensor magnitudes and orientations.

The advent of high-resolution solid-state NMR has made it possible to measure J-coupling between magnetically equivalent quadrupolar nuclei in solids. Characteristic multiplets have been observed using DOR NMR spectroscopy and have been described as originating from the reduced mixing of the total-spin eigenstates.[29] Similar experiments have also been performed using MQMAS NMR spectroscopy where computational spectrum analysis is necessary to analyze the multiplets.[38] Several *J*-resolved NMR experiments have also

been presented that are capable of providing *J* and even dipolar coupling between quadrupolar nuclei; interestingly, the result obtained depends crucially on the crystallographic symmetry of the compound.[44,47] Magnetically equivalent quadrupolar spin pairs give rise to amplified *J* splittings, yielding additional information regarding the symmetry of the molecule and facilitating the detection of smaller J-coupling constants. In static *J*/*D*-resolved experiments, Pake-like doublets are obtained, the sense of which depends on whether or not the nuclei are magnetically equivalent.[49] Although there are to date few reports regarding the use of such methods, the determination of crystallographic symmetry via the equivalence of quadrupolar spin pairs adds an interesting new dimension to structure elucidation. The methods discussed in this article may also be used to measure connectivities and internuclear distances in materials containing quadrupolar nuclei.

Acknowledgments

We acknowledge the Natural Sciences and Engineering Research Council of Canada for funding our research in this area. Acknowledgment is made to the donors of The American Chemical Society Petroleum Research Fund for partial support of this research.

Biographical Sketches

Frédéric A. Perras. b 1988. B.Sc. (Hons), 2010, University of Ottawa; PhD, 2014, University of Ottawa. Introduced to solid-state NMR spectroscopy by Prof. David L. Bryce at the University of Ottawa, with whom he pursued doctoral studies in the development of solid-state NMR spectroscopy of quadrupolar nuclei. Postdoctoral fellow with Prof. Marek Pruski at Ames Laboratory, Iowa (2015–). Approx. 20 publications. Research interests include solid-state NMR, quadrupolar nuclei, spectral simulation, and dynamic nuclear polarization.

David L. Bryce. b 1975. B.Sc. (Hons), 1998, Queen's University; PhD, 2002, Dalhousie University (with R. E. Wasylishen). Postdoctoral Fellow, Laboratory of Chemical Physics, NIH, 2003–2004 (with A. Bax). Faculty in Department of Chemistry, University of Ottawa, 2005–present. Approx. 120 publications. Research interests include solid-state NMR of low-frequency quadrupolar nuclei, NMR studies of halogen bonds, NMR studies of materials, quantum chemical interpretation of NMR interaction tensors, biomolecular NMR.

Related Articles

Dipolar and Indirect Coupling Tensors in Solids; Indirect Nuclear Spin-Spin Coupling Tensors; Magnetic Equivalence; Two-Dimensional *J*-Resolved Spectroscopy; Quadrupolar Interactions; Quadrupolar Nuclei in Solids: Influence of Different Interactions on Spectra

References

1. J. A. Pople, W. G. Schneider, and H. J. Bernstein, High-Resolution Nuclear Magnetic Resonance, McGraw-Hill: New York, 1959.
2. M. H. Levitt, Spin Dynamics, 2nd edn, John Wiley & Sons Ltd: Chichester, 2009 Chapter 14.
3. R. K. Harris, Nuclear Magnetic Resonance Spectroscopy. A Physicochemical View, Pearson Education: Harlow, 2005 Chapter 2.
4. M. Carravetta, O. G. Johannessen, and M. H. Levitt, *Phys. Rev. Lett.*, 2004, **98**, 153003.
5. M. Carravetta and M. H. Levitt, *J. Am. Chem. Soc.*, 2004, **126**, 6228.
6. M. Carravetta and M. H. Levitt, *J. Chem. Phys.*, 2005, **122**, 214505.
7. G. Pileio, M. Carravetta, E. Hughes, and M. H. Levitt, *J. Am. Chem. Soc.*, 2008, **130**, 12582.
8. M. C. D. Tayler and M. H. Levitt, *J. Am. Chem. Soc.*, 2013, **135**, 2120.
9. M. C. D. Tayler, I. Marco-Rius, M. I. Kettunen, K. M. Brindle, M. H. Levitt, and G. Pileio, *J. Am. Chem. Soc.*, 2012, **134**, 7668.
10. G. Peleio, S. Bowen, C. Laustsen, M. C. D. Tayler, J. T. Hill-Cousins, L. J. Brown, R. C. D. Brown, J. H. Ardenkjaer-Larsen, and M. H. Levitt, *J. Am. Chem. Soc.*, 2013, **135**, 5084.
11. Y. Feng, T. Theis, X. Liang, Q. Wang, P. Zhou, and W. S. Warren, *J. Am. Chem. Soc.*, 2013, **135**, 9632.
12. J. I. Musher, *J. Chem. Phys.*, 1967, **46**, 1537.
13. U. Haeberlen, in Advances in Magnetic Resonance, ed. J. S. Waugh, Academic Press: New York, 1976Supplement 1, Chapter III.
14. G. Wu and R. E. Wasylishen, *J. Chem. Phys.*, 1993, **96**, 6138.
15. G. Wu and R. E. Wasylishen, *J. Chem. Phys.*, 1994, **100**, 5546.
16. G. Wu, R. E. Wasylishen, H. Pan, C. W. Liu, J. P.Fackler Jr, and M. Shang, *Magn. Reson. Chem.*, 1995, **33**, 734.
17. E. R. Andrew, A. Bradbury, R. G. Eades, and V. T. Wynn, *Phys. Lett.*, 1963, **4**, 99.
18. H. J. Hogben, P. J. Hore, and I. Kuprov, *J. Magn. Reson.*, 2011, **211**, 217.
19. R. E. Wasylishen, S. E. Ashbrook, and S. Wimperis, NMR of Quadrupolar Nuclei in Solid Materials, Wiley & Sons Ltd: Chichester, 2012.
20. D. Iuga, C. Morais, Z. Gan, D. R. Neuville, L. Cormier, and D. Massiot, *J. Am. Chem. Soc.*, 2005, **127**, 11540.
21. M. Deschamps, F. Fayon, V. Montouillout, and D. Massiot, *Chem. Commun.*, 2006, 1924.
22. I. Hung, A.-C. Uldry, J. Becker-Baldus, A. L. Webber, A. Wong, M. E. Smith, S. A. Joyce, J. R. Yates, C. J. Pickard, R. Dupree, and S. P. Brown, *J. Am. Chem. Soc.*, 2009, **131**, 1820.
23. N. S. Barrow, J. R. Yates, S. A. Feller, D. Holland, S. E. Ashbrook, P. Hodgkinson, and S. P. Brown, *Phys. Chem. Chem. Phys.*, 2011, **13**, 5778.
24. G. Pileio, M. Carravetta, and M. H. Levitt, *Proc. Nat. Acad. Sci. USA*, 2010, **107**, 17135.
25. S. J. DeVience, R. L. Walsworth, and M. S. Rosen, *Phys. Rev. Lett.*, 2013, **111**, 173002.
26. Y. Feng, R. M. Davis, and W. S. Warren, *Nat. Phys.*, 2012, **8**, 831.
27. A. Abragam, Principles of Nuclear Magnetism, Oxford Science Publications: Oxford, 1961, 234.
28. F. A. Perras and D. L. Bryce, *J. Magn. Reson.*, 2014, **242**, 23.
29. F. A. Perras and D. L. Bryce, *J. Chem. Phys.*, 2013, **138**, 174202.
30. A. Saupe and J. Nehring, *J. Chem. Phys.*, 1967, **47**, 5459.
31. J. I. Musher, *J. Chem. Phys.*, 1967, **47**, 5460.
32. E. E. Burnell, A. J. van der Est, G. N. Patey, C. A.de Lange, and J. G. Snijders, *Bull. Magn. Reson.*, 1987, **9**, 4.
33. A. Samoson, E. Lippmaa, and A. Pines, *Mol. Phys.*, 1988, **65**, 1013.
34. K. T. Mueller, B. Q. Sun, G. C. Chingas, J. W. Zwanziger, T. Terao, and A. Pines, *J. Magn. Reson.*, 1990, **86**, 470.
35. I. Hung, A. Wong, A. P. Howes, T. Anupõld, J. Past, A. Samoson, X. Mo, G. Wu, M. E. Smith, S. P. Brown, and R. Dupree, *J. Magn. Reson.*, 2007, **188**, 256.
36. R. Siegel, T. T. Nakashima, and R. E. Wasylishen, *Chem. Phys. Lett.*, 2006, **421**, 529.

37. G. Facey, D. Gusev, R. H. Morris, S. Macholl, and G. Buntkowsky, *Phys. Chem. Chem. Phys.*, 2000, **2**, 935.
38. S. Wi and L. Frydman, *J. Chem. Phys.*, 2000, **112**, 3248.
39. L. Frydman and J. S. Harwood, *J. Am. Chem. Soc.*, 1995, **117**, 5367.
40. A. Medek, J. S. Harwood, and L. Frydman, *J. Am. Chem. Soc.*, 1995, **117**, 12779.
41. W. P. Aue, J. Karhan, and R. R. Ernst, *J. Chem. Phys.*, 1976, **64**, 4226.
42. E. L. Hahn, *Phys. Rev.*, 1950, **80**, 580.
43. E. L. Hahn and D. E. Maxwell, *Phys. Rev.*, 1951, **84**, 1246.
44. F. A. Perras and D. L. Bryce, *J. Am. Chem. Soc.*, 2013, **135**, 12596.
45. A. Lesage, M. Bardet, and L. Emsley, *J. Am. Chem. Soc.*, 1999, **121**, 10987.
46. Q. Wang, B. Hu, O. Lafon, J. Trébosc, F. Deng, and J.-P. Amoureux, *J. Magn. Reson.*, 2009, **200**, 251.
47. F. A. Perras and D. L. Bryce, *Chem. Sci.*, 2014, **5**, 2428.
48. H. Abu Ali, I. Goldberg, and M. Srebnik, *Eur. J. Inorg Chem.*, 2000, 73.
49. F. A. Perras and D. L. Bryce, *J. Phys. Chem. Lett.*, 2014, **5**, 4049.
50. P. J. Grandinetti, J. H. Baltisberger, A. Llor, Y. K. Lee, U. Werner, M. A. Eastman, and A. Pines, *J. Magn. Reson.*, 1993, **103**, 72.
51. D. Massiot, I. Farnan, N. Gautier, D. Trumeau, A. Trokiner, and J. P. Coutures, *Solid State Nucl. Magn. Reson.*, 1995, **4**, 241.
52. A. Brinkmann and M. Edén, *Can. J. Chem.*, 2011, **89**, 892.
53. S. Wi, J. W. Logan, D. Sakellariou, J. D. Walls, and A. Pines, *J. Chem. Phys.*, 2002, **117**, 7024.
54. R. W. Schurko, *Acc. Chem. Res.*, 2013, **46**, 1985.